



Starch/polyaniline nanocomposite for enhanced removal of reactive dyes from synthetic effluent

V. Janaki^a, K. Vijayaraghavan^b, Byung-Taek Oh^c, Kui-Jae Lee^c, K. Muthuchelian^d, A.K. Ramasamy^{a,*}, Seralathan Kamala-Kannan^{c,**}

^a Department of Chemistry, Periyar University, Salem 636011, Tamil Nadu, India

^b Singapore-Delft Water Alliance, National University of Singapore, 117577, Singapore

^c Division of Biotechnology, Advanced Institute of Environment and Bioscience, College of Environmental and Bioresource Sciences, Chonbuk National University, Iksan 570752, South Korea

^d Department of Bioenergy, School of Energy Environment and Natural Resources, Madurai Kamaraj University, Madurai 625021, Tamil Nadu, India

ARTICLE INFO

Article history:

Received 30 March 2012

Received in revised form 13 June 2012

Accepted 3 July 2012

Available online 13 July 2012

Keywords:

Biosorption

Dye bath

Nanocomposite

Polyaniline

Reactive dyes

Starch

ABSTRACT

Starch/polyaniline nanocomposite was synthesized by chemical oxidative polymerization of aniline and was subsequently analyzed for dye removal from aqueous solution. Batch experiment results showed that nanocomposite removed 99% of Reactive Black 5, 98% of Reactive Violet 4, and decolorized 87% of dye bath effluent. The Toth isotherm model better described single component equilibrium adsorption, whereas the modified Freundlich model showed satisfactory fit for dye bath. In kinetic modeling, single system followed pseudo-second-order and dye bath followed the modified pseudo-first-order model. Fourier transform infrared spectroscopy pattern of the nanocomposite showed the participation of aromatic, amino, hydroxyl, and carboxyl groups. The results indicate that starch/polyaniline nanocomposite can be used as an effective adsorbent for removal of dyes from textile effluents.

© 2012 Elsevier Ltd. All rights reserved.

1. Introduction

Dyes are extensively used in several industries such as textile, leather tanning, food processing, cosmetics, electroplating, paper, and pharmaceutical industries. Several classes of synthetic dyes (over 7×10^5 metric tons) are produced worldwide every year for industrial purposes and about 5–10% of this quantity is released into the ecosystem along with wastewater. The amount of dye in wastewater depends on the type of dye used in industry; it varies from 2% for basic dyes and 10 to 50% for reactive dyes (Al-Degs, El-Barghouthi, El-Sheikh, & Walter, 2008; Dafale, Rao, Meshram, & Wate, 2008).

Reactive dyes are characterized by azo bonds ($N=N$), and the color of the dye is due to the associated chromophores. It is most commonly used in textile industries because of simple dyeing procedure and covalent binding with cellulose fibers. However, hydroxyl ions present in the dye bath can compete with the cellulose substrate, resulting in a higher percentage of hydrolyzed

dyes which can no longer react with the cellulose fiber. Thus, approximately 50% of the initial dye concentration is present in the reactive dye bath, giving rise to a highly colored effluent (Al-Degs et al., 2008; Vijayaraghavan, Won, & Yun, 2009). Many reactive dyes are toxic to biotic communities in aquatic ecosystem (Papic, Koprivanac, Bozic, & Metes, 2004). Therefore, there is a necessity to treat reactive dye effluents before their discharge into ecosystem.

Numerous physical, chemical, and biological techniques have been developed for the removal of reactive dyes from effluents. Among the techniques, adsorption is one of the most efficient methods because of its low cost and easy operational conditions. Materials such as egg shell, peanut hull, activated carbon, and microorganisms have been used as an adsorbent for the removal of reactive dyes from effluents (Elkady, Ibrahim, & El-Latif, 2011; Jadhav, Kalyani, Telke, Phugare, & Govindwar, 2010; Mona, Kaushik, & Kaushik, 2011; Tanyildizi, 2011; Vijayaraghavan & Yun, 2008a). The size of these adsorbents varies from submicron to micron and has large internal porosities to ensure adequate surface area for adsorption. However, the diffusion limitation had decreased the adsorption rate and interactions between the adsorbent and adsorbate. Hence, it is important to develop a novel adsorbent with a limited diffusion resistance. The development of nanotechnology in various fields has widened the application in wastewater treatment. Compared to the micron-sized conventional adsorbents,

* Corresponding author. Tel.: +91 427 2345271.

** Corresponding author. Tel.: +82 63 850 0842; fax: +82 63 850 0834.

E-mail addresses: drakramasamy@yahoo.in (A.K. Ramasamy), kannan@jbnu.ac.kr (S. Kamala-Kannan).

nano-sized carriers possess quite good performance due to the high specific surface area with little internal diffusion resistance (Chang, Chang, & Chen, 2006).

Starch, an inexpensive natural renewable polysaccharide, has been widely used in various fields because of its inherent properties (Lu, Xiao, & Xu, 2009). However, native starch has limited dye adsorption capacity because of weak adsorbing functional groups in its backbone (Xing, Liu, Xu, & Liu, 2012). Several approaches have been made to modify starch as a potential adsorbent for dyes (Cheng, Ou, Li, Li, & Xiang, 2009; Cheng, Xiang, Li, & Zhang, 2011; Renault, Morin-Crini, Gimbert, Badot, & Crini, 2008; Xu, Wang, Wu, Wang, & Li, 2006). However, practical operation and high cost reduced the application of modified starch in large scale. Thus, starch based composites have been prepared for the removal of dyes from aqueous solution (Chang, Chen, & Jiao, 2010; Chen, Shang, Fang, & Diao, 2011; Wang, Xiang, Cheng, & Li, 2010; Xing et al., 2012).

In the last decades, there has been considerable interest in the synthesis of conducting/biopolymer composite that comprise different chemical and biological polymers. This becomes an important area of composite research because of its application in material science and environmental sciences. Recently, polyaniline/chitosan (Pn/Ch) and bacterial extracellular polysaccharides/polyaniline (Pn/EPS) composites are used for the removal of reactive dyes from aqueous solution (Janaki et al., 2012a, 2012b). The high expensive nature of chitosan, series of steps in preparation of bacterial extracellular polysaccharides, and diffusion limitation of the composites may decrease the dye adsorption capacity. Thus, it is noteworthy to prepare a nanocomposite of two polymers starch and polyaniline. However, to our knowledge starch/polyaniline (St/Pn) nanocomposite has never been used as an adsorbent for the removal of dyes. Hence, the objectives of the present study were to

(i) synthesize and characterize St/Pn nanocomposite, (ii) evaluate the potential of St/Pn nanocomposite for the removal of reactive dyes from aqueous solution and treatment of reactive dye bath, (iii) assess the experimental variables affecting optimal removal of dyes, and (iv) explore adsorption isotherms and kinetic models to identify the possible mechanism of dye removal.

2. Materials and methods

2.1. Materials

Food quality grade of maize starch was dried at 105 °C before using. Aniline monomer was purchased from Sigma–Aldrich (St. Louis, MO) and it was distilled under reduced pressure before use. Dyes such as Reactive Black 5 (RB) and Reactive Violet 4 (RV) and the auxiliary chemicals were also purchased from Sigma–Aldrich.

2.2. Synthesis and characterization of St/Pn nanocomposite

St/Pn nanocomposite was prepared according to Janaki et al. (2012b) with minor modification. Briefly, 4% (w/v) starch was suspended in nanopure purified water (conductivity = 18 $\mu\text{S}/\text{m}$, TOC < 3 ppb, Barnstead, Waltham, MA, USA) and the solutions was stirred to form a homogenous solution. To this, about 0.01 M aniline dissolved in 1 M HCl was added drop wise and stirred for 15 min. Ammonium peroxydisulfate (4.4 g) solution in 1 M HCl was added drop wise with constant stirring at 5 °C. The molar ratio of oxidant to monomer was 1:2. Later, the solution mixture was stirred for another 5 h and kept in a refrigerator overnight. The resulting greenish-black precipitate was separated by centrifugation and washed with nanopure water and methanol until the filtrate become colorless. The resulting composite was freeze-dried

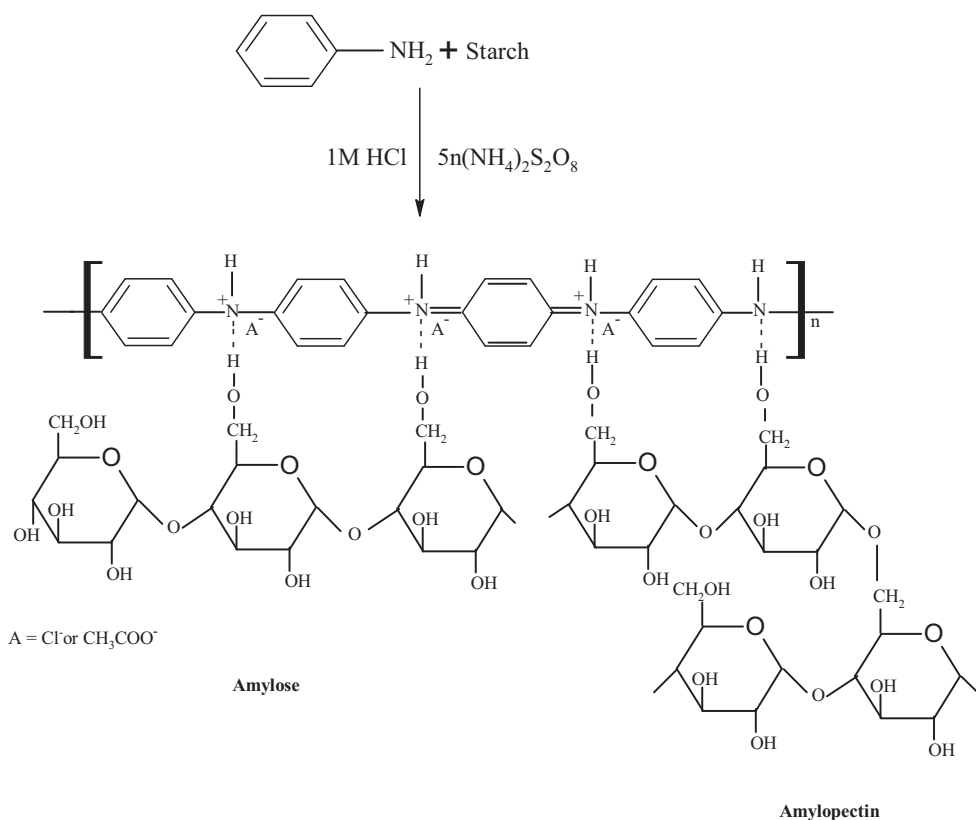


Fig. 1. Polymerization mechanism of St/Pn nanocomposite.

under vacuum at -80°C for 24 h and used for the further studies. Fig. 1 shows the mechanism of polymerization between starch and Pn.

Morphological features of St/Pn nanocomposite were obtained from scanning electron microscopy (SEM) using a JEOL JSM-6400 microscope (Tokyo, Japan). X-ray diffractograms (XRD) were obtained using a Cu K α incident beam ($\lambda = 0.1546\text{ nm}$), monochromated by a nickel filtering wave at a tube voltage of 40 kV and tube current of 30 mA. The scanning was done in the region of 2θ from 4° to 60° at $0.04^{\circ}/\text{min}$ with a time constant of 2 s. The Fourier transform infrared spectroscopy (FTIR) spectra of the St/Pn nanocomposite were obtained using a Perkin-Elmer FTIR spectrophotometer (CA, USA) in the diffuse reflectance mode at a resolution of 4 cm^{-1} in KBr pellets.

2.3. Preparation of synthetic dye bath effluent

Synthetic dye bath effluent was prepared according to Alaton, Balcioğlu, and Bahnemann (2002) with minor modification. The chemical constituents present in the dye bath effluent comprised of RB (1.0 mM), RV (1.0 mM), sodium chloride (710 mM), sodium carbonate (122 mM), sodium hydroxide (13 mM), and acetic acid (13 mM). RB and RV dyes have vinylsulfone anchor groups, which react with the cellulose anions through the nucleophilic addition under alkaline condition. Thus, to ensure that all the chemicals in the dye stuffs were 100% hydrolyzed, the dye bath was boiled for 3 h and allowed to cool for 12 h. The composition of the synthetic dye bath effluent was assumed to be 20% of the original dye stuff and 100% of all the auxiliary chemicals present in the exhausted dye bath.

2.4. Experimental procedure

Batch adsorption was performed in Erlenmeyer flasks containing 100 ml of the desired dye concentration or synthetic dye effluent with 0.06 g of St/Pn nanocomposite. If necessary, the pH of the solution was initially adjusted and controlled using 0.1 N HCl or NaOH. The flasks were subjected to shaking at a constant speed of 150 rpm at 25°C in a shaking incubator. After the attainment of equilibrium, the samples were centrifuged at 9000 rpm for 10 min and the total dye concentration was analyzed using a UV-vis spectrophotometer (UV-1800 Shimadzu, Japan) at the respective wavelength maxima (597, 577, and 584 nm for RB, RV, and dye bath effluent, respectively) after appropriate dilution.

2.5. Recovery studies

In order to investigate the desorption efficiency of reactive dyes from St/Pn nanocomposite, 0.12 g of St/Pn nanocomposite was introduced into 200 ml of RB (0.5 mM), RV (0.5 mM), and dye bath effluent [RB (0.5 mM), RV (0.5 mM), sodium chloride (355 mM), sodium carbonate (61 mM), sodium hydroxide (6.5 mM), and acetic acid (6.5 mM)] at 25°C . As the adsorption reaches the equilibrium, St/Pn nanocomposite was separated by centrifugation (9000 rpm for 10 min) and washed gently with nanopure water to remove unadsorbed dyes. Later, the St/Pn nanocomposite was freeze-dried under vacuum at -80°C for 24 h and used for desorption studies. The nanocomposite (0.06 g) was agitated (150 rpm) with 100 ml of 0.1 M NaOH at 25°C for predetermined equilibrium time of the adsorption process. After desorption, the supernatant was centrifuged, with the remaining procedure being the same as for the sorption experiments.

2.6. Data evaluation

The dye removal in single dye system was calculated from the difference between the dye concentrations in the supernatant using the following mass balance equation:

$$Q = \frac{V(C_0 - C_f)}{M} \quad (1)$$

where Q is the dye uptake (mg g^{-1}), C_0 and C_f are the initial and final dye concentrations in the solution (mol L^{-1}), respectively, V is the volume of the solution (L), and M is the mass of St/Pn nanocomposite (g).

Single dye adsorption isotherms were modeled using the Langmuir, Freundlich, and Toth models, which can be represented as follows:

Langmuir model:

$$Q = \frac{Q_{\max} b C_f}{1 + b C_f} \quad (2)$$

Freundlich model:

$$Q = K_F (C_f)^{1/n_F} \quad (3)$$

Toth model:

$$Q = \frac{Q_{\max} b_T C_f}{[1 + (b_T C_f)^{1/n_T}]^{n_T}} \quad (4)$$

where Q is the equilibrium dye uptake (mmol g^{-1}), Q_{\max} is the maximum adsorption capacity of the adsorbent (mmol g^{-1}), b is the Langmuir equilibrium constant (L mmol^{-1}), K_F is the Freundlich constant (mmol g^{-1}) (L mmol^{-1}) $^{1/n_F}$, n_F is the Freundlich model exponent, b_T is the Toth model constant (L mmol^{-1}), and n_T is the Toth model exponent.

The experimental kinetic data were described using pseudo-first and second-order kinetics, which can be expressed in their nonlinear form as follows:

Pseudo-first-order model:

$$q_t = q_e [1 - \exp(-k_1 t)] \quad (5)$$

Pseudo-second-order model:

$$q_t = \frac{q_e^2 k_2 t}{1 + q_e k_2 t} \quad (6)$$

where q_e is the amount of dye sorbed at equilibrium (mmol g^{-1}), q_t is the amount of dye sorbed at time t (mmol g^{-1}), k_1 the rate constant of pseudo-first-order model (min^{-1}) and k_2 the rate constant of pseudo-second-order model ($\text{g mmol}^{-1} \text{ min}^{-1}$).

To represent the dye removal in effluent, two parameters viz. percentage removal and extent of decolorization were used (Vijayaraghavan et al., 2009). The percentage removal can be represented as follows:

$$\text{Removal (\%)} = \frac{Abs_i - Abs_f}{Abs_i} \times 100 \quad (7)$$

The extent of decolorization, Q_D (L g^{-1}), can be calculated from:

$$Q_D = \frac{V(Abs_i - Abs_f)}{M} \quad (8)$$

where Abs_i and Abs_f are the initial and final absorbance of the dye, respectively, V is the effluent volume (L) and M is the mass of the St/Pn nanocomposite used (g).

A modified form of the Freundlich model was used to describe the isotherm data of dye bath effluent, which is a plot of the final absorbance versus the extent of decolorization, which can be represented as follows:

$$Q_D = K_F (Abs_f)^{1/n_F} \quad (9)$$

The dye bath kinetic data were described using the pseudo-first-order kinetic equation, which can be represented in its nonlinear form as follows:

$$Q_{Dt} = Q_{De}[1 - \exp(-k_1 t)] \quad (10)$$

where Q_{De} is the extent of decolorization at equilibrium (L g^{-1}), Q_{Dt} is the extent of decolorization at time t (L g^{-1}), and k_1 is the first order equilibrium rate constant (min^{-1}). All the model parameters were evaluated by nonlinear regression using the Sigma Plot (version 8.0, SPSS, USA) software. Duplicate experiments were carried out for all the operating variables studied and only the average values were considered. Blank experiments were carried out with dye effluent solution (no adsorbent) concurrently to ensure that the sorption of dye on the walls of flasks was negligible.

3. Results and discussion

3.1. Characterization of St/Pn nanocomposite

Representative electron micrograph of the synthesized St/Pn nanocomposite is depicted in Fig. 2. The particles were irregular in shape and mostly present in aggregates. The surface of the particles was rough due to polymerization of aniline (Saikia, Banerjee, Konwar, & Kumar, 2010), providing a good possibility for dyes to be trapped and adsorbed. The size of the particles was varied from 70 to 90 nm. FTIR analysis was performed to study the functional groups present in St/Pn nanocomposite, and the results are presented in Fig. 3. The characteristic broad peaks at $3359\text{--}3353\text{ cm}^{-1}$ and $3187\text{--}3228\text{ cm}^{-1}$ could be assigned to O–H and N–H stretching vibration of polymeric compounds (Naumann, Helm, & Labischinski, 1991). The bands at 2958, 2560, 1969, and 1558 cm^{-1} could be ascribed to N–H bending, and a peak at 1479 cm^{-1} was assigned as C–C stretching vibration of benzenoid ring (Saikia et al., 2010). The peaks at 1299 and 1123 cm^{-1} were due to C–N and C–H stretching vibrations of benzene ring (Zareh, Moghadam, Azariyan, & Sharifian, 2011). In addition, the spectrum showed the presence of carboxyl (1242 cm^{-1}), alkane (504 cm^{-1}), and aromatic (878 and 796 cm^{-1}) groups from starch and polyaniline, respectively. The results confirmed that starch is effectively activated by superfluos acids. The inter-molecular hydrogen bonds were broken in the composite and more hydrogen groups become freely accessible for interactions with dye molecules.

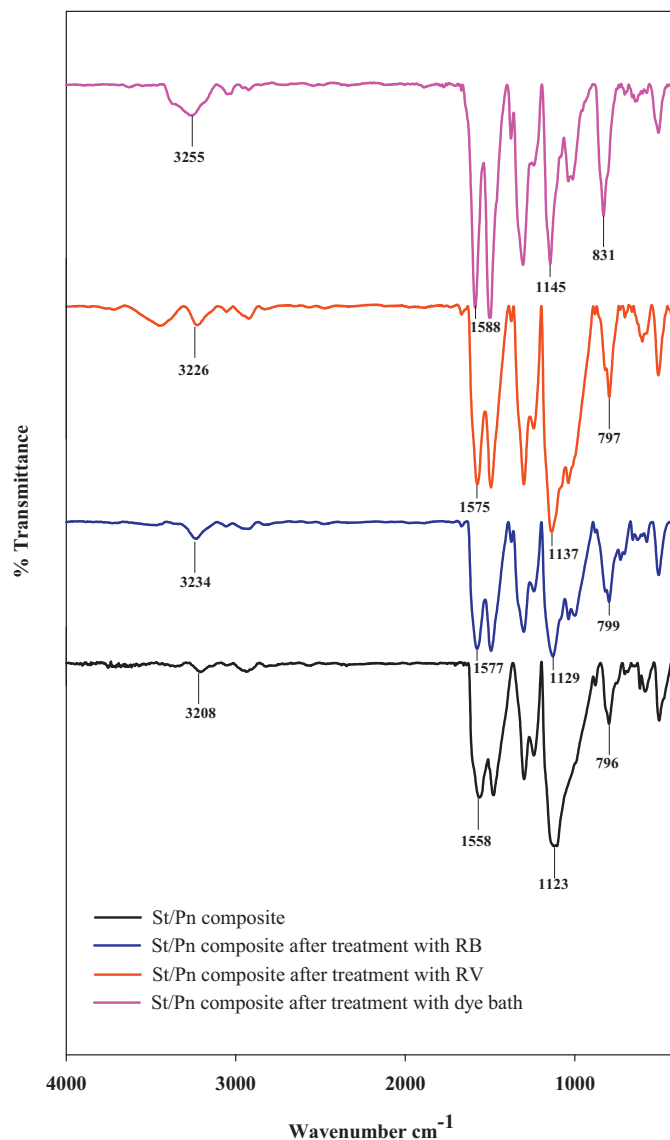


Fig. 3. FTIR spectra of St/Pn nanocomposite before and after treatment with Reactive Black, Reactive Violet, and reactive dye bath effluent.

The XRD pattern of the synthesized St/Pn nanocomposite is shown in Fig. 4. The results indicate that the nanocomposite had highly ordered crystal structure which is expected to have high adsorption properties. The diffraction peaks at $2\theta = 20.4^\circ$, 25.4° , and 26.2° were assigned to the emeraldine polyaniline (Janaki et al., 2012b; Zareh et al., 2011). The peak $2\theta = 25.4^\circ$ is corresponding to the periodicity parallel and perpendicular to polyaniline chains. The starch exhibited characteristic peaks at $2\theta = 15.28^\circ$ and 23.5° . The results are consistent with the previous study reporting the highly ordered crystal structure of St/Pn nanocomposite (Zareh et al., 2011).

3.2. Single solute adsorption system

3.2.1. Effect of pH and mechanism of adsorption

The pH is one of the important factors that affect the interaction between the adsorbent and adsorbate. Numerous studies reported that degree of ionization process of the dye molecules, surface charge of adsorbent, and chemistry of dye solution are highly influenced by pH of the effluent (Kyzas & Lazaridis, 2009; Salem, 2010). Therefore, the removal of dyes (RB and RV) was evaluated

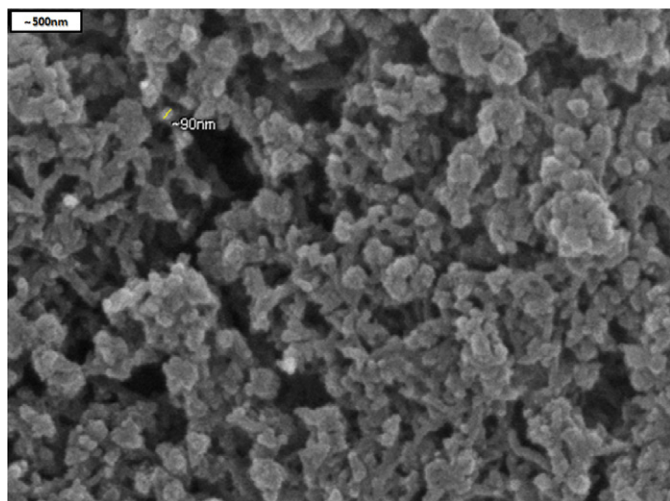


Fig. 2. SEM micrograph of St/Pn composite. The surface of the nanocomposite was rough due to polymerization of aniline.

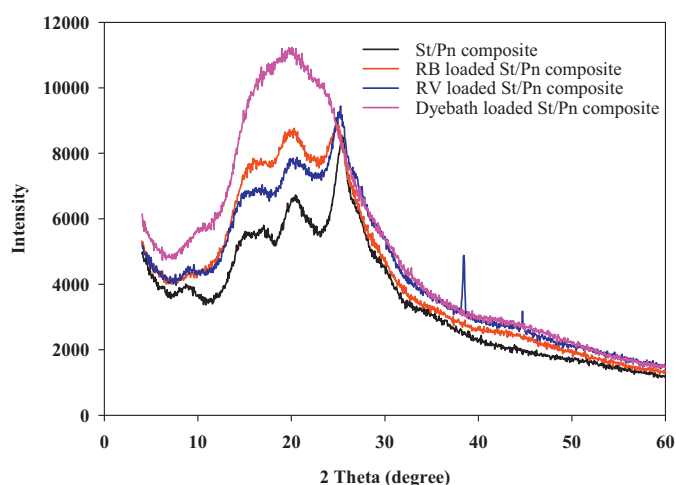


Fig. 4. XRD pattern of St/Pn nanocomposite before and after treatment with Reactive Black, Reactive Violet, and reactive dye bath effluent.

at different pH and the results are presented in Fig. 5a. The results revealed that the uptake of RB and RV onto St/Pn nanocomposite was higher in the case of acidic solutions than those in neutral and alkaline conditions. The maximum removal of dyes (99% of RB and 98% of RV) was observed at pH 3 and minimum removal (65% of RB

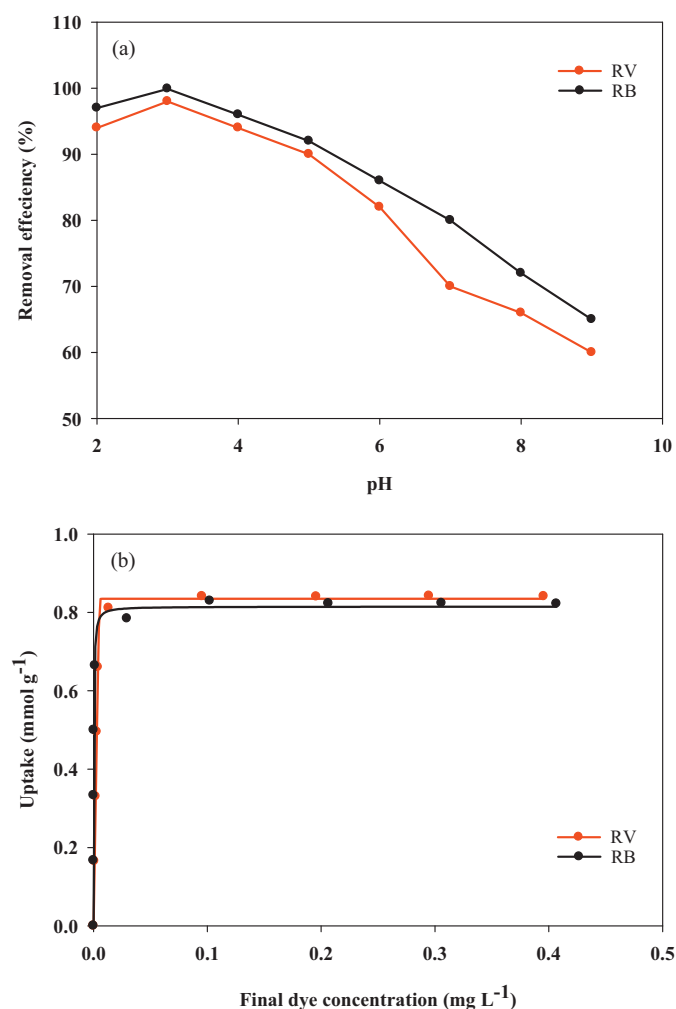


Fig. 5. (a) Effect of pH on removal of Reactive Violet and Reactive Black and (b) Toth model plots for Reactive Violet and Reactive Black.

and 60% of RV) was observed at pH 9. The higher adsorption behavior of St/Pn polymer matrix under the acidic condition is explained by the following mechanism:

- Under acidic condition, the nitrogen atom present in the constituent polymer is protonated according to the following reaction:



- Simultaneously, in aqueous solution, the reactive dye molecule is dissociated and converted into dye anions.



The reactive dye anions are migrated from solution to the surface of the St/Pn polymer matrix. As a result, the adsorption occurs through the electrostatic interaction between the two counterions.

However, as the pH increases (4–8) deprotonation of nitrogen atom occurs, leading to the depletion of active sites in the polymer skeleton. Therefore, the interaction of St/Pn nanocomposite with the dye molecule is hindered and consequently results in the lower uptake. Similar observation has been reported for the removal of various dyes using polyaniline composites (Janaki et al., 2012b; Salem, 2010).

3.2.2. Adsorption isotherm investigation

The equilibrium adsorption isotherm is of fundamental importance in the design of the adsorption systems. The shape of an isotherm denotes the affinity of dye molecules and possible mechanism of adsorption. In the present study, the experimental data were fitted to the Langmuir, Freundlich, and Toth isotherm models, and their constants are presented in Table 1. The Langmuir isotherm is based on the assumption that adsorption takes place at specific homogenous sites within the adsorbent (Runping, Pan, Zhaohui, Zhenhui, & Mingsheng, 2008). It is then assumed that all the sites are energetically equivalent and once these sites are occupied, no further adsorption can take place at that site. Also, Langmuir isotherm helps to estimate the affinity (b) between the adsorbent and adsorbate. The higher b value of RB (3692.4 L mmol^{−1}) when compared with RV (422.40 L mmol^{−1}) could be due to the steeper isotherm exhibited by RB. The Q_{max} value observed for RB and RV were 0.8180 (811.30 mg g^{−1}) and 0.7863 mmol g^{−1}

Table 1

Adsorption isotherm and kinetic model constants for adsorption of RB and RV onto St/Pn nanocomposite.

Isotherm/kinetic models	Parameters	RB	RV
Langmuir	Q_{max} (mmol g ^{−1})	0.8180	0.7863
	b (L mmol ^{−1})	3692.4	422.40
	R^2	0.9890	0.9638
Freundlich	K_F (mmol g ^{−1})	0.9799	1.0455
	$(\text{L mmol}^{-1})^{1/n}$		
	n_F	0.1127	0.1339
Toth	R^2	0.8787	0.8142
	Q_{max} (mmol g ^{−1})	0.8148	0.8348
	b_T (L mmol ^{−1})	3291.2	197.60
Pseudo-first order	n_T	0.9015	0.0450
	R^2	0.9893	0.9992
	Q_e (mmol g ^{−1})	0.5240	0.6760
Pseudo-second order	K_1 (min ^{−1})	0.1254	0.0517
	R^2	0.9837	0.9779
	Q_e (mmol g ^{−1})	0.5731	0.8311
Pseudo-second order	K_2 (g mmol ^{−1} min ^{−1})	0.3642	0.0675
	R^2	0.9967	0.9876

(578.39 mg g⁻¹), respectively. The adsorption capacity values for both the reactive dyes were superior to those in the previous published works. The cationic starch intercalated clay matrix exhibited the Q_{\max} value of 112.4 mg g⁻¹ for Brilliant Blue X-BR (Xing et al., 2012). Dithiocarbamate-modified starch exhibits the Q_{\max} value of 0.807, 0.451, 0.359, 0.443, and 0.449 mmol g⁻¹ for Acid Orange 7, Acid Orange 10, Acid Green 25, Acid Black 1 and Acid Red 18, respectively (Cheng et al., 2011). Polyaniline microspheres exhibit the Q_{\max} value of 154.56 mg g⁻¹ for Methyl Orange (Ai, Jiang, & Zhang, 2010). Polyaniline/chitosan composite exhibited the Q_{\max} value of 322.58, 357.14, and 303.03 mg g⁻¹ for the removal of CR, CBB and RBBR, respectively (Janaki et al., 2012a). Several reasons may explain the high adsorption potential of the St/Pn nanocomposite as compared with other polysaccharide composites; the freely accessible hydrogen atoms present in the St/Pn composite may increase the adsorption rate of dyes. Alternatively, the nitrogen constituents present in the polyaniline (Salem, 2010; Zareh et al., 2011), limited internal diffusion resistance and high surface area of the nanocomposite may increase the adsorption potential of the composite. The correlation coefficients (R^2) observed for RB and RV were 0.9890 and 0.9638, respectively. The high correlation coefficient for both the reactive dyes predicted monolayer coverage.

The Freundlich equation is an empirical equation which assumes that adsorption energy exponentially decreases on completion of the sorptional centers of an adsorbent. This model exhibits slightly inferior correlation coefficient (R^2) (0.8787 for RB and 0.8142 for RV) as compared to the Langmuir isotherm. The K_F and n_F represent the affinity and binding capacity between the adsorbate and the adsorbent. The higher K_F and n_F was observed for the dyes RB and RV showing the high affinity and binding capacity between the dye molecules and polymer composite.

Numerous studies reported that the three-parameter model, the Toth model, could improve the fitness of adsorption isotherm data (Gimbert, Morin-Crini, Renault, Badot, & Crini, 2008; Vijayaraghavan et al., 2009). The Toth isotherm is derived from potential theory and it is useful to explain adsorption process in heterogeneous system (Runping et al., 2008). It assumes a quasi-Gaussian energy distribution, and reactive sites are considered to have an adsorption lower than the maximum adsorption energy. The involvement of additional parameter in the Toth model leads to better description of adsorption isotherms in many instances (Vijayaraghavan & Yun, 2008a). By comparing the experimental data and predicted curves, it was found that both the Toth and Langmuir isotherms can describe reasonably well. In particular, three-parameter model provides a high correlation coefficient ($R^2 = 0.989$ for RB and $R^2 = 0.999$ for RV) than the Langmuir model ($R^2 = 0.989$ for RB and $R^2 = 0.964$ for RV) and able to describe the experimental data well for both the reactive dyes. The predicted Toth curves for both the reactive dyes are shown in Fig. 5b. This result showed that adsorption system was heterogeneous. The results are in agreement with the previous study on the treatment of complex Remazol dye effluent using sawdust- and coal-based activated carbons (Vijayaraghavan et al., 2009).

3.2.3. Adsorption kinetics and modeling

The kinetic study provides information about the sorption mechanism and sorption characteristics of adsorption system. Therefore the kinetic experiments were carried out in fixed dye concentration (1.0 mM) for both the reactive dyes RB and RV (Fig. 6). Rapid uptake was observed during the first 10 min and gradually decreased with laps of time until equilibrium. The increased activity at initial stage was especially due to the availability of more active sites present in the polymer matrix, on occupancy of these sites the uptake was slower and reaches the equilibrium at 40 min. The two kinetic models, pseudo-first-order and pseudo-second-

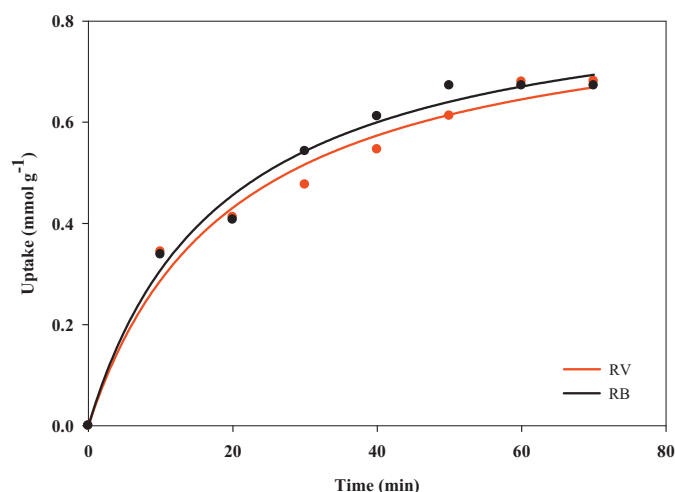


Fig. 6. Pseudo second-order model predicted curves for Reactive Black and Reactive Violet.

order models, were used to investigate the kinetics involved in the adsorption of reactive dyes onto St/Pn nanocomposite. The correlation coefficient and the important kinetic parameters are listed in Table 1.

The pseudo-first-order kinetic model did not provide the satisfactory fit to the experimental data. The calculated equilibrium adsorption capacities (q_e) do not agree with the experimental (q_e) value. The difference in the q_e values could be due to a time lag, possibly as a result of formation of boundary layer on the surface of the polymer or by the external resistance controlling the adsorption process (McKay, Ho, & Ng, 1999). In addition regression coefficient ($R^2 = 0.984$ for RB and $R^2 = 0.978$ for RV) values deviated slightly away from unity suggesting that pseudo-first-order model was not an appropriate model for describing the kinetics involved in the adsorption of reactive dyes (RB and RV) onto St/Pn nanocomposite. Hence, the data were further tested with pseudo-second-order model. The correlation coefficients of both the dyes ($R^2 = 0.997$ for RB and $R^2 = 0.987$ for RV) found closer to unity, and in addition the calculated q_e values were closer to the experimental values. The predicted pseudo-second-order curves for both the reactive dyes are shown in Fig. 6. The results indicate that adsorption of two reactive dyes onto St/Pn nanocomposite follows pseudo-second-order model and chemisorption being the rate-controlling step. The results are in agreement with the previous study reported that the adsorption of brilliant blue X-BR on the cationic starch intercalated clay composite matrix (Xing et al., 2012).

3.3. Treatment of dye effluent

3.3.1. Influence of pH in dye removal

It has been established that different salts and auxiliary chemicals reduced the dye removal rate in textile effluents (Aksu, 2005). Hence, the efficiency of St/Pn nanocomposite was assessed for dye bath containing RB, RV, and other auxiliary chemicals. Although the composite exhibited maximum adsorption for dyes (RB and RV) at pH 3, dye bath experiments were conducted at pH 5 because of carbonate effervescence at strong acidic pH (2–4). The St/Pn nanocomposite exhibited 87% removal of dyes in dye bath effluent. The decreased removal rate was due to salts and auxiliary chemicals present in dye bath, which reduce the dissociation rate of dye molecules and the interaction between the dye molecule and St/Pn nanocomposite (Mahmoodi, Hayati, Arami, & Lan, 2011; Zhu, Jiang, & Xiao, 2010).

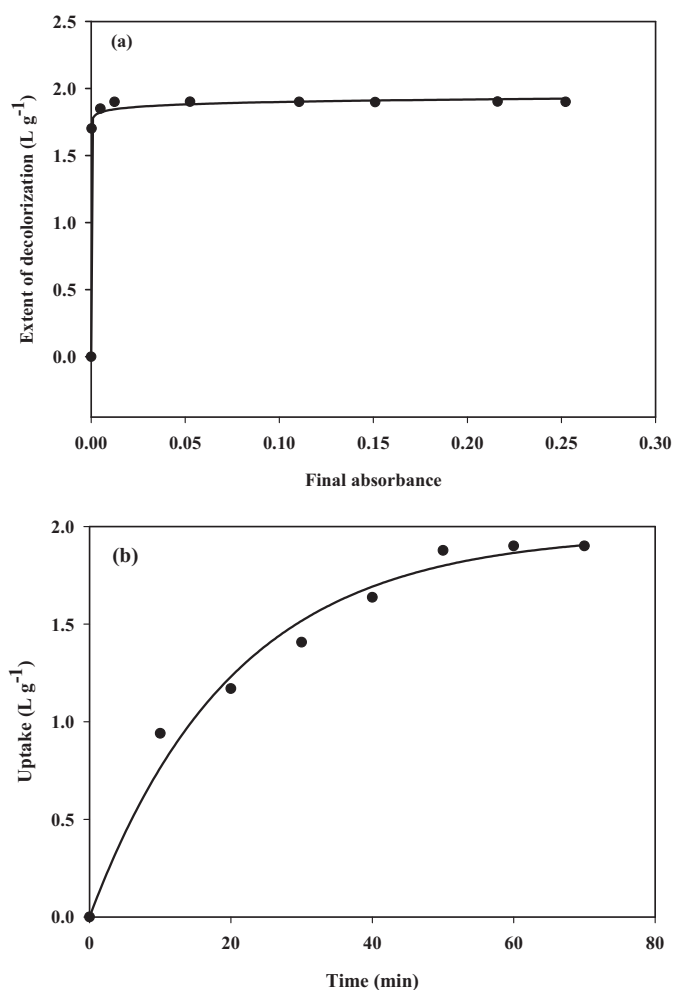


Fig. 7. Isotherm and kinetic plots for reactive dye bath adsorption onto St/Pn nanocomposite: (a) Freundlich isotherm and (b) pseudo first-order kinetics.

3.3.2. Isotherms and kinetics

A modified form of the Freundlich model was used to investigate the adsorption isotherms for dye bath. The concentration term in the conventional model (Freundlich, 1907) was replaced by an absorbance term, which is indicative of the color. The high correlation coefficient ($R^2 = 0.998$) indicated that the adsorption isotherm of dye bath followed the Freundlich model. The predicted Freundlich isotherm curve is shown in Fig. 7a, which was in good accord with the experimental data. The K_F and n_F values were 1.9616 L g^{-1} and 0.0139 , respectively. The kinetics of dye bath effluent onto St/Pn nanocomposite was analyzed using the modified pseudo first-order kinetic equation, and the predicted curve is shown in Fig. 7b. Values of Q_{De} , k_1 , and R^2 were calculated as 1.9680 L g^{-1} , 0.0491 min^{-1} , and 0.981 , respectively. The correlation coefficient was closer to unity, and the difference between the experimental Q_{De} and calculated Q_{De} was very less, indicating the better fit of pseudo first-order kinetic model.

3.4. FTIR and XRD studies

To understand the role of functional groups involved in dye binding, FTIR spectra for RV, RB, and dye bath-treated St/Pn nanocomposites were examined, and the results are presented in Fig. 3. The disappearance of peaks at 3357 and 1242 cm^{-1} in RV, RB, and dye bath-treated samples indicates the participation of hydroxyl and carboxyl groups. The major shift in peaks at 3208 , 2560 , 1669 , and 1558 cm^{-1} showed the contribution of amino

group in adsorption of dyes (Janaki et al., 2012b). A minor shift in peak at 1479 cm^{-1} indicated the role of carbon group in the removal of dyes. Similar trend was observed on the adsorption of dyes onto several adsorbent (Janaki et al., 2012b; Zhang et al., 2009). The XRD profile of RV, RB, and dye bath laden St/Pn nanocomposite is presented in Fig. 4. The results revealed that highly ordered crystalline nature of the nanocomposite changing into amorphous nature after adsorption of dyes. The changes in the phase of adsorbent indicate that the dye molecules diffuse into micropores and macropores, and adsorb by ionic interaction. The results are consistent with the previous studies reporting changes in Pn/EPS composite after adsorption of reactive dyes (Janaki et al., 2012b).

3.5. Desorption

Desorption study helps to elucidate the mechanism and recovery of the adsorbent. To investigate the application of St/Pn nanocomposite for several cycles and to confirm the process by which dye molecules adsorbed onto the nanocomposite, sequential sorption–desorption experiments were carried out for five cycles. The selection of eluant is an important factor as it depends on the type and mechanism of adsorbent. Since the nanocomposite showed maximum adsorption of RV and RB under strong acidic condition (pH 3), then it is logical to unbind the dyes in the more basic solution (0.1 M NaOH) (Vijayaraghavan & Yun, 2008b). Therefore (0.1 M NaOH) was used as eluant for desorption studies. Under the more basic condition, the negative charged sites increases and it causes the elution of dye anions from the polymeric surface due to electrostatic repulsion. The elution efficiency for RV was 93% and RB was 94.2%. However, the elution efficiency in dye bath loaded nanocomposite was 89.4% only. The decreased elution could be due to salts and auxiliary chemical present in the dye bath. The results have further confirmed the ionic interaction between the dye molecules and St/Pn nanocomposite (Janaki et al., 2012b). Moreover, a negligible reduction (4%) in sorption capacity of nanocomposite was observed. Hence, the adsorbent can be regenerated and reused for several cycles.

3.6. Advantages of using St/Pn composite in adsorption process

In tune with the need for sustainable ecosystem, researches have been focused toward the eco-friendly methods for the treatment of industrial wastes. Although the benefits of adsorption process are well known, the use of eco-friendly adsorbent is important for sustainable development. Various agro industrial wastes, natural/modified polysaccharides, and biological materials are used as an adsorbent for the removal of dyes from aqueous solution. However, using St/Pn nanocomposite for the removal of dyes has several advantages than other adsorbents. The advantages are (i) starch is an inexpensive and easily available natural polysaccharide, (ii) because of nanosize the composite may have high surface area and limited diffusion resistance, (iii) high adsorption efficiency reduced the adsorbent dosage and thereby the generation of secondary sludge, (iv) preparation of the St/Pn composite is easy compared with Pn/EPS composite, and (v) the composite is eco-friendly.

4. Conclusion

The following are the suggested conclusion based on the results of the present study

- To the best of our knowledge this is first study to report the application of St/Pn nanocomposite for the treatment reactive dyes and simulated dye bath effluent.
- St/Pn nanocomposite was synthesized by chemical oxidative polymerization using ammonium peroxydisulfate as initiator.

XRD studies showed that the synthesized nanocomposite had characteristic features of both starch and polyaniline. The presence of carboxyl (1242 cm^{-1}), alkane (504 cm^{-1}), and aromatic (878 and 796 cm^{-1}) groups from starch may increase the adsorption capacity of the composite.

- The superfluous acids broken inter-molecular hydrogen bonds in the starch, consequently more hydrogen groups become freely accessible for interactions with dye molecules.
- The present study showed that St/Pn nanocomposite has significantly removed RB (99%) and RV (98%) from aqueous solution. The removal rate for both the reactive dyes was superior to those in the previous published works. The hydrogen bonding and electrostatic interaction between polymer and dyes were responsible for the enhanced adsorption.
- The dye bath effluent that contains RB, RV, and auxiliary chemicals was also significantly decolorized by the St/Pn nanocomposite. However, a minor difference in dye decolorization rate was observed between single component and dye bath.
- The adsorption isotherms were modeled using Langmuir, Freundlich and Toth models. Toth model describe the equilibrium data of RB and RV with high correlation coefficient. The adsorption kinetics was found to follow pseudo-second order rather than first order model.
- The ionic interaction between the dye molecules and St/Pn nanocomposite was confirmed by the FTIR and desorption studies. The crystalline nature of the nanocomposite altered to amorphous nature due to adsorption.
- The simple and ease of synthesis, and relatively high adsorption capacity nature indicate that St/Pn nanocomposite can be effectively used for the treatment of reactive dye effluents.

References

- Ai, L., Jiang, J., & Zhang, R. (2010). Uniform polyaniline microspheres: A novel adsorbent for dye removal from aqueous solution. *Synthetic Metals*, 160, 762–767.
- Aksu, Z. (2005). Application of biosorption for the removal of organic pollutants: A review. *Process Biochemistry*, 40, 997–1026.
- Alaton, I. A., Balcioglu, I. A., & Bahnemann, D. W. (2002). Advance oxidation of a reactive dye bath effluent: Comparison of O_3 , H_2O_2 /UV-C and TiO_2 /UV-A processes. *Water Research*, 36, 1143–1154.
- Al-Degs, Y. S., El-Barghouti, M. I., El-Sheikh, A. H., & Walter, G. M. (2008). Effect of solution pH, ionic strength, and temperature on adsorption behavior of reactive dyes on activated carbon. *Dyes and Pigments*, 77, 16–23.
- Chang, Y. C., Chang, S. W., & Chen, D. H. (2006). Magnetic chitosan nanoparticles: Studies on chitosan binding and adsorption of Co(II) ions. *Reactive and Functional Polymers*, 66, 335–341.
- Chang, X., Chen, D., & Jiao, X. (2010). Starch-derived carbon aerogels with high-performance for sorption of cationic dyes. *Polymer*, 51, 3801–3807.
- Chen, M., Shang, T., Fang, W., & Diao, G. (2011). Study on adsorption and desorption properties of the starch grafted p-tert-butyl-calix[n]arene for butyl Rhodamine B solution. *Journal of Hazardous Materials*, 185, 914–921.
- Cheng, R., Ou, S., Li, M., Li, Y., & Xiang, B. (2009). Ethylenediamine modified starch as biosorbent for acid dyes. *Journal of Hazardous Materials*, 172, 1655–1670.
- Cheng, R., Xiang, B., Li, Y., & Zhang, M. (2011). Application of dithiocarbamate-modified starch for dyes removal from aqueous solutions. *Journal of Hazardous Materials*, 188, 254–260.
- Dafale, N., Rao, N. N., Meshram, S. U., & Wate, S. R. (2008). Decolorization of azo dyes and simulated dye bath wastewater using acclimatized microbial consortium—biostimulation and halo tolerance. *Bioresource Technology*, 99, 2552–2558.
- Elkady, M. F., Ibrahim, A. M., & El-Latif, M. M. A. (2011). Assessment of the adsorption kinetics, equilibrium and thermodynamic for the potential removal of reactive red dye using eggshell biocomposite beads. *Desalination*, 278, 412–423.
- Freundlich, H. (1907). Ueber die Adsorption in Loesungen. *Zeitschrift fur Physikalische Chemie*, 57, 385–470.
- Gimbert, F., Morin-Crini, N., Renault, F., Badot, P. M., & Crini, G. (2008). Adsorption isotherm models for dye removal by cationized starch-based material in a single component system: Error analysis. *Journal of Hazardous Materials*, 157, 34–46.
- Jadhav, J. P., Kalyani, D. C., Telke, A. A., Phugare, S. S., & Govindwar, S. P. (2010). Evaluation of the efficacy of a bacterial consortium for the removal of color, reduction of heavy metals, and toxicity from textile dye effluent. *Bioresource Technology*, 101, 165–173.
- Janaki, V., Oh, B. T., Shanthi, K., Lee, K. J., Ramasamy, A. K., & Kamala-Kannan, S. (2012). Polyaniline/chitosan composite: An eco-friendly polymer for enhanced removal of dyes from aqueous solution. *Synthetic Metals*, 162, 974–980.
- Janaki, V., Oh, B. T., Vijayaraghavan, K., Kim, J. W., Kim, S. A., Ramasamy, A. K., et al. (2012). Application of bacterial extracellular polysaccharides/polyaniline composite for the treatment of Remazol effluent. *Carbohydrate Polymers*, 88, 1002–1008.
- Kyzas, G. Z., & Lazaridis, N. K. (2009). Reactive and basic dyes removal by sorption onto chitosan derivatives. *Journal of Colloid and Interface Science*, 331, 32–39.
- Lu, D. R., Xiao, C. M., & Xu, S. J. (2009). Starch-based completely biodegradable polymer materials. *Express Polymer Letters*, 6, 366–375.
- Mahmoodi, N. M., Hayati, B., Arami, M., & Lan, C. (2011). Adsorption of textile dyes on *Pine cone* from colored wastewater: Kinetic, equilibrium and thermodynamic studies. *Desalination*, 268, 117–125.
- McKay, G., Ho, Y. S., & Ng, J. C. Y. (1999). Biosorption of copper from wastewaters: A review. *Separation and Purification Methods*, 28, 87–125.
- Mona, S., Kaushik, A., & Kaushik, C. P. (2011). Biosorption of reactive dye by waste biomass of *Nostoc linckia*. *Ecological Engineering*, 37, 1589–1594.
- Naumann, D., Helm, D., & Labischinski, H. (1991). Microbiological characterization by FT-IR spectroscopy. *Nature*, 351, 81–82.
- Papic, S., Koprivanac, N., Bozic, A. L., & Metes, A. (2004). Removal of some reactive dyes from synthetic wastewater by combined Al(III) coagulation/carbon adsorption process. *Dyes and Pigments*, 62, 291–298.
- Renault, F., Morin-Crini, N., Gimbert, F., Badot, P., & Crini, G. (2008). Cationized starch based material as a new ion-exchanger adsorbent for the removal of C.I. Acid Blue 25 from aqueous solution. *Bioresource Technology*, 99, 7573–7586.
- Runping, H., Pan, H., Zhao, H., Zhenhui, Z., & Mingsheng, T. (2008). Kinetics and isotherms of neutral red adsorption on peanut husk. *Journal of Environmental Sciences*, 20, 1035–1041.
- Saikia, J. P., Banerjee, S., Konwar, B. K., & Kumar, A. (2010). Biocompatible novel starch/polyaniline composites: Characterization, anti-cytotoxicity and antioxidant activity. *Colloids and Surfaces B: Biointerfaces*, 81, 158–164.
- Salem, M. A. (2010). The role of polyaniline salts in the removal of direct blue 78 from aqueous solution: A kinetic study. *Reactive and Functional Polymers*, 70, 707–714.
- Tanyildizi, M. S. (2011). Modeling of adsorption isotherms and kinetics of reactive dye from aqueous solution by peanut hull. *Chemical Engineering Journal*, 168, 1234–1240.
- Vijayaraghavan, K., Won, S. W., & Yun, Y. S. (2009). Treatment of complex Remazol dye effluent using sawdust- and coal-based activated carbons. *Journal of Hazardous Materials*, 167, 790–796.
- Vijayaraghavan, K., & Yun, Y. S. (2008a). Bacterial biosorbents and biosorption. *Biotechnology Advances*, 26, 266–291.
- Vijayaraghavan, K., & Yun, Y. S. (2008b). Competition of Reactive red 4, Reactive orange 16 and Basic blue 3 during biosorption of Reactive blue 4 by polysulfone-immobilized *Corynebacterium glutamicum*. *Journal of Hazardous Materials*, 153, 478–486.
- Wang, Z., Xiang, B., Cheng, R., & Li, Y. (2010). Behaviors and mechanism of acid dyes sorption onto diethylenetriamine-modified native and enzymatic hydrolysis starch. *Journal of Hazardous Materials*, 183, 224–232.
- Xing, G., Liu, S., Xu, Q., & Liu, Q. (2012). Preparation and adsorption behavior for Brilliant Blue X-BR of the cost-effective cationic starch intercalated clay composite matrix. *Carbohydrate Polymers*, 87, 1447–1452.
- Xu, S., Wang, J., Wu, R., Wang, J., & Li, H. (2006). Adsorption behaviors of acid and basic dyes on crosslinked amphoteric starch. *Chemical Engineering Journal*, 117, 161–167.
- Zareh, E. N., Moghadam, P. N., Azariyan, E., & Sharifian, I. (2011). Conductive and biodegradable polyaniline/starch blends and their composites with polystyrene. *Iranian Polymer Journal*, 20, 319–328.
- Zhang, Z., Xia, S., Wang, X., Yang, A., Xu, B., Chen, L., et al. (2009). A novel biosorbent for dye removal: Extracellular polymeric substance (EPS) of *Proteus mirabilis* TJ-1. *Journal of Hazardous Materials*, 163, 279–284.
- Zhu, H. Y., Jiang, R., & Xiao, L. (2010). Adsorption of an anionic azo dye by chitosan/kaolin/ $\gamma\text{-Fe}_2\text{O}_3$ composite. *Applied Clay Science*, 48, 522–526.